Scientific Research Publishing

Journal of Geoscience and Environment Protection, 2023, 11, 28-57
https://www.scirp.org/journal/gep
ISSN Online: 2327-4344
ISSN Print: 2327-4336

Biosorptive Removal of Lead Ions from Aqeuous Stream by Using Leaves, Stems and Roots of *Momordica charantia* Biomass

Badar Khan[1], Afifah Jabeen Khan[2]

[1]The University of Lahore, Lahore, Pakistan
[2]Government College University Lahore (GCUL), Lahore, Pakistan
Email: badarkhan1023@gmail.com, afifahjabeen@gmail.com

How to cite this paper: Khan, B., & Khan, A. J. (2023). Biosorptive Removal of Lead Ions from Aqeuous Stream by Using Leaves, Stems and Roots of *Momordica charantia* Biomass. *Journal of Geoscience and Environment Protection, 11,* 28-57.
https://doi.org/10.4236/gep.2023.1112003

Received: October 26, 2023
Accepted: December 5, 2023
Published: December 8, 2023

Copyright © 2023 by author(s) and Scientific Research Publishing Inc.
This work is licensed under the Creative Commons Attribution International License (CC BY 4.0).
http://creativecommons.org/licenses/by/4.0/

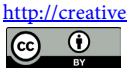

Open Access

Abstract

Water pollution is one of the most important issues of the 21st century. It takes place when the pollutants are being entered into a water reservoir without any treatment. Heavy metals are one of the major harmful pollutants that exist in the water; therefore, it is necessary to remove these toxic metals to keep our environment safe. Biosorption is an ecofriendly and economical technique for the elimination of these toxic metals from polluted water. In this research work roots, stems, and leaves of *Momordica charantia* (Bitter gourd) were used as biosorbent for the elimination of Pb (II) ions from aqueous solution. Many different parameters such as metal ion solution pH, biomass dosage, initial metal ions concentration and contact time were optimized in the batch experiments. The calculated results revealed that biosorption of Pb (II) was maximum at solution pH 5, biosorbent dosage of 0.1 g and 100 ppm of initial metal ions concentration within 240 minutes of contact time. *M. charantia's* leaves showed the highest level of lead biosorption capacity (47.62%), followed by stems (42.36%) and roots (38.47%). The Freundlich isotherm and pseudo-second order kinetics model fitted well for the analytical data. The results indicated that *Momordica charantia* is an effective biosorbent for Pb (II) ions elimination from wastewater.

Keywords

Biosorption, Lead (Pb), Heavy Metal, Environment Protection, Wastewater Treatment, *Momordica charantia* Biomass

1. Introduction

Polluted water is a notable challenge for all the countries of the world. Due to the

quick non-sustainable industrial, urban development, farming and other framework system, water contamination is rapidly increasing and consequently causing harmful diseases and restricting freshwater accessibility all over the world (Vishwanath et al., 2017). Globally, approximately 2.5 billion are living without the proper sanitation facilities (UNICEF, 2008). Mainly, water pollutants produced by anthropogenic activities are heavy metals, microorganisms, pathogens, nutrients, inorganic compounds, organic material, pesticides, and oxygen consuming compounds (Akpor & Muchie, 2011).

Heavy metals (HM) are amongst the most poisonous pollutants on the earth (Ashraf et al., 2011). They cannot be degraded or destroyed. Though heavy metals are naturally present as a trace constituent of the marine environment, due to industrial sewerage, agriculture wastes, geological and mining projects, their levels have been increased (Sprocati et al., 2006). Heavy metals are fatal due to their bioaccumulation in the living organisms. Bioaccumulation refers to the accumulation of any foreign chemical in a living organism (fish for example) over the period of time, compared to the concentration of that chemical in the surroundings (Abbas et al., 2014). If toxic metals accumulated in biological organism, then it will enter in the food chain. Some of these pollutants sometimes find their way into the human system through the food chain. The fish is the most likely organism to bio-accumulate by heavy metals because they are at the start of food chain and can become the vector for humans (Bawuro et al., 2018).

Lead is among the most toxic heavy metals present in the water. It is occurred naturally and generally present in very small amounts in our earth's deposit. It is present in almost every part of the earth, the soil, the atmosphere, and the water. There are several lead products used in our homes and surroundings including ceramics, pipes and plumbing materials, batteries, gasoline, toys, paints, folk medicines, and cosmetics (Chaney & Mielke, 1986). Though lead has some beneficial uses, it can be very toxic and dangerous for our environment, leading to lead toxicity to humans, animals, and plants. There are some natural sources of lead exposure, but major sources of lead come from anthropogenic activities (Gurugubelli et al., 2013).

There are various techniques that have been established and used for the elimination of heavy metals in the past decades, such as chemical precipitation, ion exchange, ion flotation, membrane filtration or electrodialysis. But there are some disadvantages of conventional techniques being utilized for the removal of heavy metals, such as greater costs, lower efficiency, and unwanted residue generation (Beni & Esmaeili, 2020). Hence, there is a need for bioremediation which has greater removal efficiency and relatively inexpensive. This led to the discovering of new techniques for the removal of heavy metals from polluted water and pay focuses on biosorptive removal process.

Biosorption can remove heavy metals even at very low concentration by using different types of dead biological mass. These biomasses have special abilities to attach heavy metals (Ahluwalia & Goyal, 2007). Generally, the cell wall composition of several plants, algae, fungi, and bacteria, has the characteristics to per-

form this phenomenon (Volesky, 1990). Primarily, the cell wall is mostly composed of polysaccharides, proteins, and lipids, which have different functional groups on it, such as hydroxyl, carboxyl, amino, ester, and carbonyl group. These functional groups are of great importance in combining metal ions present in the solution (Talaro & Talaro, 2002).

In this study the biosorption of lead ions was compared by using leaves (LMC), stems (SMC) and roots (RMC) of *Momordica charantia,* known as balsam pear or karela, is a tropical vegetable, a common food in Asian cuisine and is often used in ancient medicine as a medicine for diabetes. In Ayurveda, bitter gourd is used as a tonic, stomachic, stimulant, emetic, taming agent, cathartic, and substitute. Bitter gourd has long been used in various primitive Asian systems of medicine. Like most bitter plants, bitter gourd improves digestion (Munichandran et al., 2016). To investigate the biosorption of lead ions, different experiments were carried out using bitter melon leaves, stems, and roots powder as a biosorbent. The optimization of the biosorbents was carried out using FTIR. The effects of different process parameters such as pH, biomass dose, contact time and initial metal concentration on the removal of lead ions from aqueous solution were observed and optimized.

2. Materials and Methods

Bitter Gourd (*Momordica charantia*) utilized in this research was collected from its native habitats located in Narowal District, Pakistan **Figure 1**. The gathered plant's biomass was initially submerged in the freshwater and then thoroughly washed under the running tap water to throw away all the dirt present on it. The roots, stems and leaves were cut out from the plants and after that they were separately cleaned with distilled water. The cleaned *Momordica charantia* parts; roots (RMC), stems (SMC) and leaves (LMC) were sun dried separately for 3 days. After drying, all the parts individually grounded into the powder form with the help of mixy and sieved from a nest of sieves to get 20 - 40 mesh size of LMC, SMC and RMC, as shown in **Figures 2-4**, respectively. The prepared

Figure 1. *Momordica charantia* complete plant (Roots, Stems, Leaves and Fruit).

Figure 2. *Momordica charantia* leaves powder.

Figure 3. *Momordica charantia* stems powder.

Figure 4. *Momordica charantia* roots powder.

fine powder samples were separately sealed in the plastic bags which were used in the adsorption experiments.

2.1. Chemicals

1) Lead Nitrate ($Pb(NO_3)_2$)
2) Hydrochloric Acid (HCl)
3) Sodium Hydroxide (NaOH)
4) Distilled Water (DW)
5) Lead Reference Solution for AAS

Lead Nitrate (molecular formula = $Pb(NO_3)_2$; molecular weight = 331.2 g/mol) was obtained from Sigma-Aldrich Chemicals. Stock solution of 1000 ppm of Pb

(II) ions was prepared by dissolving 1.598 g of the $Pb(NO_3)_2$ in 1 L of distilled deionized water. Experimental solutions of Pb (II) were prepared by using dilution formula ($C_1V_1 = C_2V_2$) from the stock solution. All the other reagents used in this research were of analytical grade.

2.2. Biosorption Experiments

Batch kinetic adsorption experiments were conducted to find and compare the biosorption capacity of RMC, SMC and LMC from synthetic aqueous solution of Pb (II) ions. The effect of experimental parameters such as metal ion solution pH (3, 4, 5, 6, 7 and 8), biosorbent dosage (0.1, 0.2, 0.3, 0.4 and 0.5 g), initial metal ion concentration (25, 50, 100, 200 and 400 ppm) and contact time (15, 30, 60, 120, 240, 480 and 1440 minutes) were investigated for the sorption of Pb (II) ions onto the LMC, SMC and RMC biomass. All the experiments were performed in 250 mL Erlenmeyer flasks having 100 mL of diluted aqueous solution of Pb (II) ions, covered with aluminum foil, and placed on the orbital shaker at the continuous speed of 120 rpm. After 24 Hours, the flasks were removed from the orbital shaker and filtered the experimental solution with the help of Whatman filter paper. The filtrates were analyzed in the AAS instrument to find the remaining quantity of Pb (II) ions present in the solution and residues were stored in Eppendorf tube for FTIR analysis.

2.3. Metal Analysis

After 24 hours biosorption, the concentration of the metal ions was estimated through an atomic absorption spectrophotometer. The results of lead ions adsorbed by roots, stems and leaves were quantified by using metal uptake formula:

$$q_e = \frac{\left(C_i - C_e\right) \times \left(V/1000\right)}{m} \quad [1]$$

where,

q_e represents the amount of metal uptake (mg/l).

C_i represents the initial lead ion concentration (mg/l).

C_e represents the final lead ion concentration (mg/l).

V represents the volume of solution (dm^3).

m represents the mass of adsorbent (g).

Percentage removal of Pb (II) ions was calculated with the help of general formula:

$$\%\ R = \frac{C_i - C_e}{C_i} \times 100 \quad [2]$$

where,

$\%\ R$ is the percentage of metal ion adsorbed from initial concentration.

C_i is the initial concentration of lead (mg/l) at the start of biosorption.

C_e is the final concentration of the lead (mg/l) after the biosorption experiment.

3. Results and Discussions

In this research, the powder of leaves (LMC), stems (SMC) and roots (RMC) *of Momordica charantia* (Bitter gourd) was used for the adsorption of Pb (II) ions. The following parameters effects on the biosorption of Pb (II) ions were studied.

1) Effect of metal ion solution pH
2) Effect of biosorbent dose
3) Effect of initial metal ions concentration
4) Effect of contact time

The effects of all these parameters on biosorption of Pb (II) ions are described below:

3.1. Effect of Metal Ion Solution pH

The effect of the pH on the biosorption capacity of Pb (II) ions on the biosorbent, as shown in Table 1. The bisorption of Pb (II) ions increased from 3 - 5 pH and significantly decreased with the further increase of pH. LMC, SMC and RMC showed maximum percentage removal of Pb (II) at pH 5.0; 47.24% for LMC, 42.36% for SMC and 38.47% for RMC as shown in Figures 5-7, respectively.

Table 1. Effect of pH on the adsorption capacity (q_e) and percentage removal of Pb (II) ions by LMC, SMC and RMC.

	pH	C_i (mg/L)	C_e (mg/L)	$C_i - C_e$	q_e (mg/g)	% Removal
LMC	3	100	90.39	9.61	9.61	9.61
	4	100	85.45	14.55	14.55	14.55
	5	100	52.76	47.24	47.24	47.24
	6	100	75.39	24.61	24.61	24.61
	7	100	84.85	15.15	15.15	15.15
	8	100	91.45	8.55	8.55	8.55
SMC	3	100	87.15	12.85	12.85	12.85
	4	100	76.56	23.44	23.44	23.44
	5	100	57.64	42.36	42.36	42.36
	6	100	72.42	27.58	27.58	27.58
	7	100	82.44	17.56	17.56	17.56
	8	100	90.04	9.96	9.96	9.96
RMC	3	100	90.02	9.98	9.98	9.98
	4	100	82.49	17.51	17.51	17.51
	5	100	61.53	38.47	38.47	38.47
	6	100	79.76	20.24	20.24	20.24
	7	100	84.8	15.20	15.20	15.20
	8	100	91.21	8.79	8.79	8.79

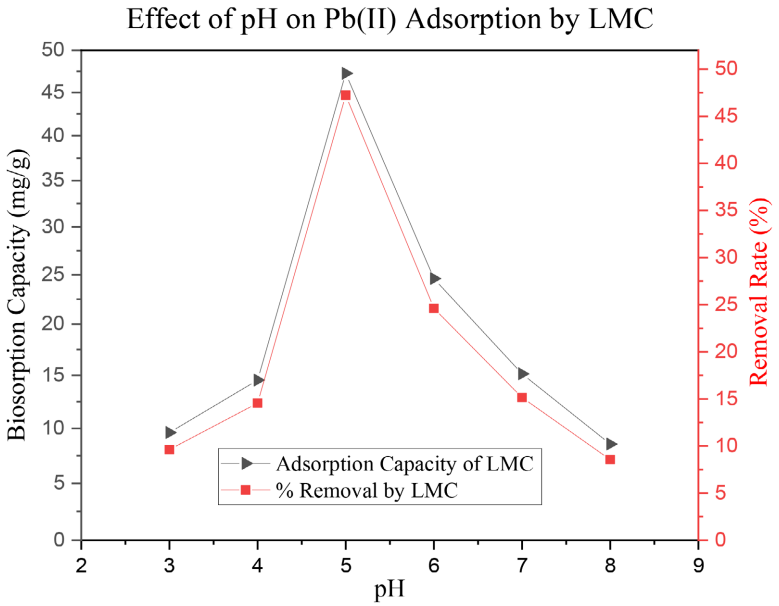

Figure 5. Effect of pH on the adsorption of Pb (II) by *Momordica charantia* leaves powder (LMC) (Experimental conditions: C_i = 100 ppm, biosorbent dosage = 0.1 g, mixing rate = 120 rpm and contact time = 24 hours).

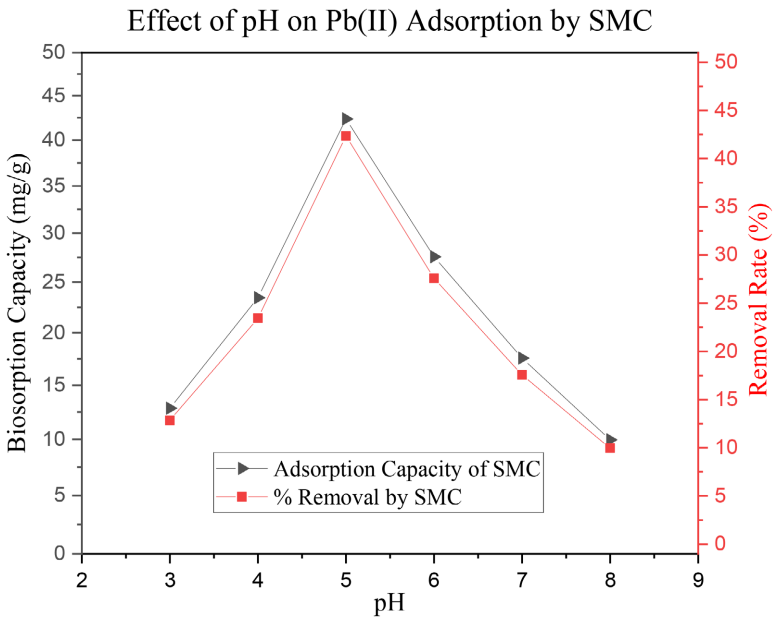

Figure 6. Effect of pH on the adsorption of Pb (II) by *Momordica charantia* stems powder (SMC) (Experimental conditions: C_i = 100 ppm, biosorbent dosage = 0.1 g, mixing rate = 120 rpm and contact time = 24 hours).

Similar trend has been reported for the Pb (II) ions elimination by utilizing *Mangifera indica* biomass (Nadeem et al., 2016).

At lower pH, the active sites of biomass are most probably to be protonated which resulted into poor metal uptake (Nadeem et al., 2016). At pH 5 for bitter gourd (LMC, SMC and RMC) biomass maximum biosorption occurred. The decreased in biosorption on more than the optimum pH 5.0 was based upon

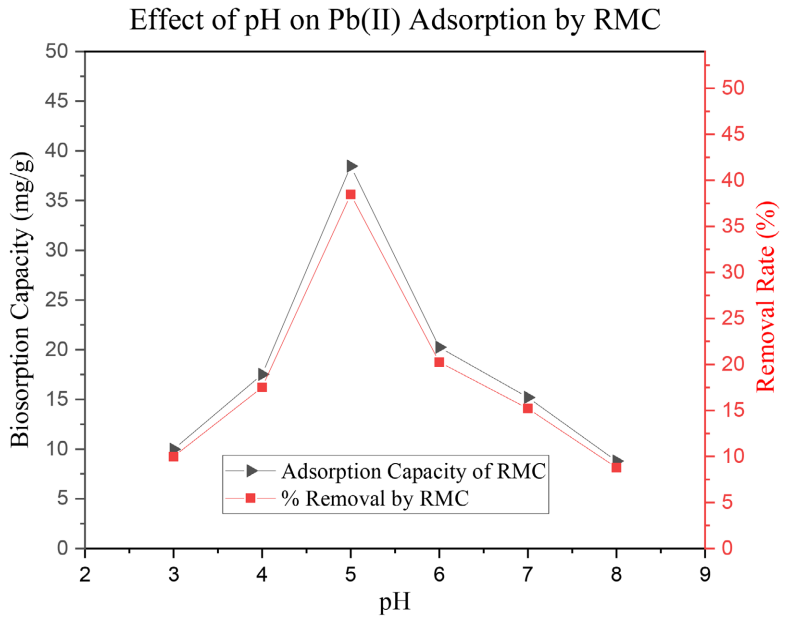

Figure 7. Effect of pH on the adsorption of Pb (II) by *Momordica charantia* roots powder (RMC) (Experimental conditions: C_i = 100 ppm, biosorbent dosage = 0.1 g, mixing rate = 120 rpm and contact time = 24 hours).

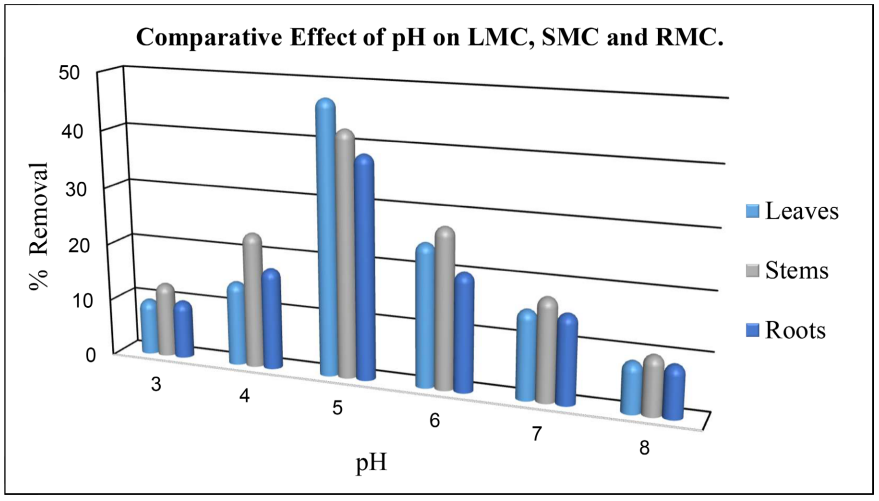

Figure 8. Comparison of percentage removal (%) of LMC, SMC and RMC on pH.

unavailability of surface for adsorption and metal hydroxide and other ligand complexes formation remarkably lessen the quantity of metal ions adsorbed at high pH (Vijayaraghavan & Yun, 2008).

In comparison among LMC, SMC and RMC, LMC (47.24%) showed the greatest percentage removal of Pb (II) ions followed by SMC (42.36%) and then RMC (38.47%) as shown in the **Figure 8**.

3.2. Effect of Biosorbent Dose

The metal uptake decreased with the increase of biomass dose from 0.1 to 0.5 g, as shown in **Table 2**. The LMC, SMC and RMC showed the maximum percentage

removal at 0.1 g biomass dose 46.45%, 41.64%, and 37.67%, respectively, as shown in Figures 9-11. Then the biosorption efficiency decreased gradually by

Table 2. Effect of biomass dose on the adsorption capacity (q_e) and percentage removal of Pb (II) ions by LMC, SMC and RMC.

	Biomass Dose (g)	C_i (mg/L)	C_e (mg/L)	$C_i - C_e$	q_e (mg/g)	% Removal
LMC	0.1	100	53.55	46.45	46.45	46.45
	0.2	100	61.3	38.7	19.35	38.70
	0.3	100	68.06	31.94	10.64	31.94
	0.4	100	72.44	27.56	6.89	27.56
	0.5	100	81.79	18.21	3.64	18.21
SMC	0.1	100	58.36	41.64	41.64	41.64
	0.2	100	65.74	34.26	17.13	34.26
	0.3	100	67.3	32.7	10.90	32.70
	0.4	100	71.33	28.67	7.16	28.67
	0.5	100	80.76	19.24	3.84	19.24
RMC	0.1	100	62.33	37.67	37.67	37.67
	0.2	100	74.51	25.49	12.74	25.49
	0.3	100	76.58	23.42	7.80	23.42
	0.4	100	82.38	17.62	4.40	17.62
	0.5	100	85.72	14.28	2.85	14.28

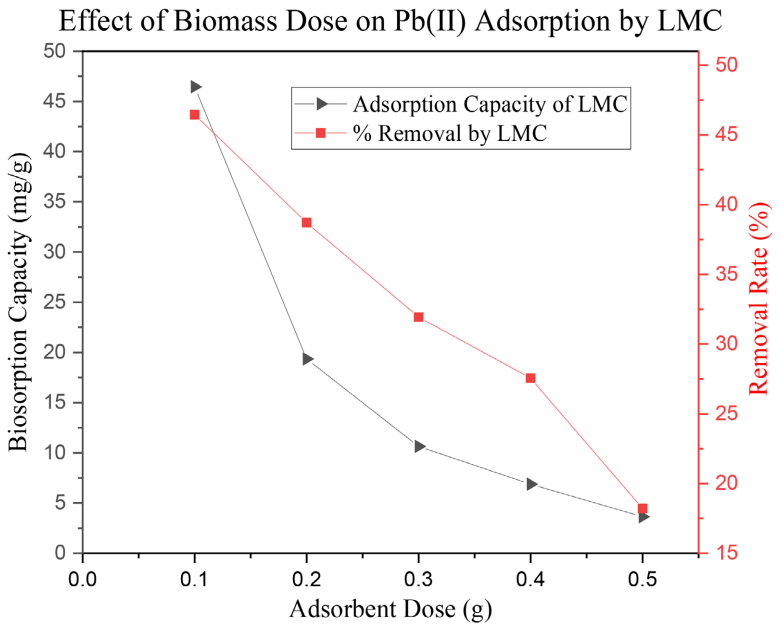

Figure 9. Effect of biomass dosage on the biosorption of Pb (II) by *Momordica charantia* leaves powder (LMC) (Experimental conditions: C_i = 100 ppm, pH = 5.0, mixing rate = 120 rpm and contact time = 24 hours).

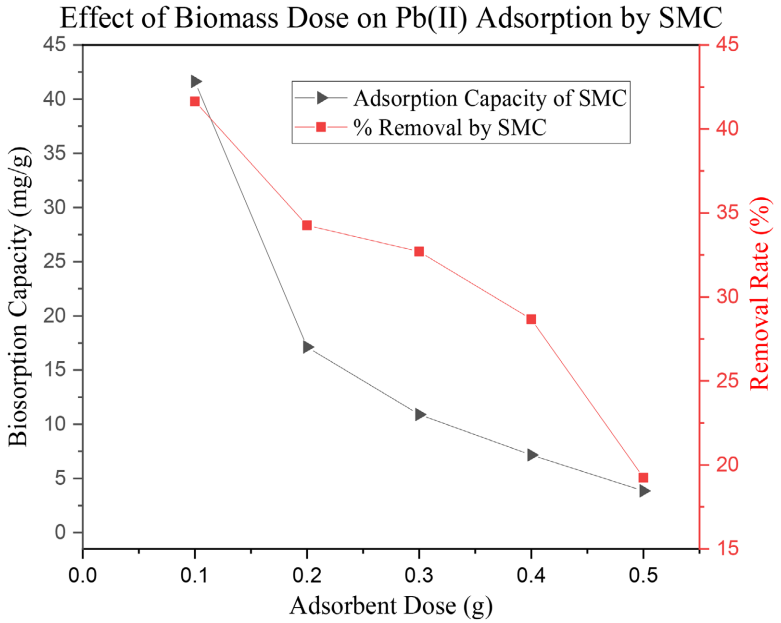

Figure 10. Effect of biomass dosage on the biosorption of Pb (II) by *Momordica charantia* stems powder (SMC) (Experimental conditions: C_i = 100 ppm, pH = 5.0, mixing rate = 120 rpm and contact time = 24 hours).

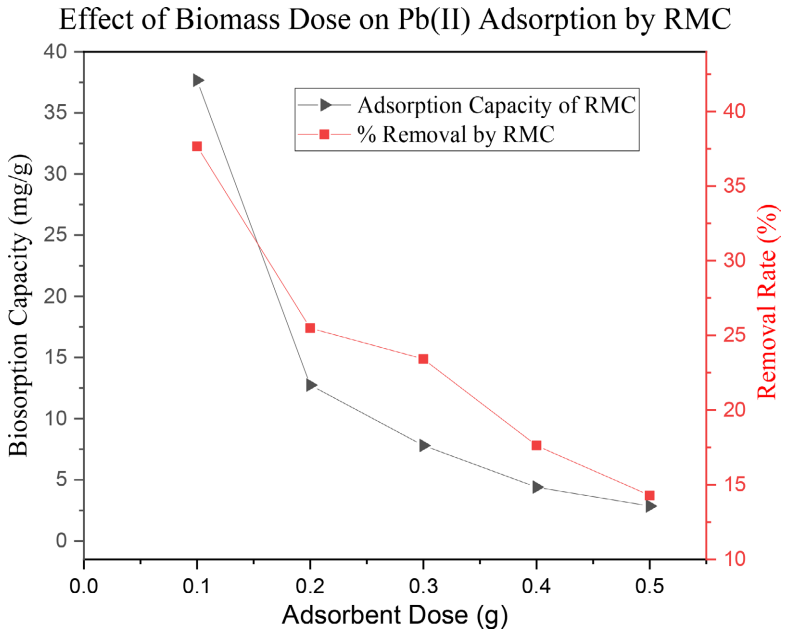

Figure 11. Effect of biomass dosage on the adsorption of Pb (II) by *Momordica charantia* roots powder (RMC) (Experimental conditions: C_i = 100 ppm, pH = 5.0, mixing rate = 120 rpm and contact time = 24 hours).

increasing the biomass dose and minimum removal observed at 0.5 g; 18.21% for LMC, 19.24% for SMC and 14.28% for RMC was recorded. Similar trends of continuous decrease in the adsorption capacity (q_e) and percentage removal have been demonstrated and discussed in many researched works (Ali et al., 2018; Manzoor et al., 2019; Padmavathy et al., 2016).

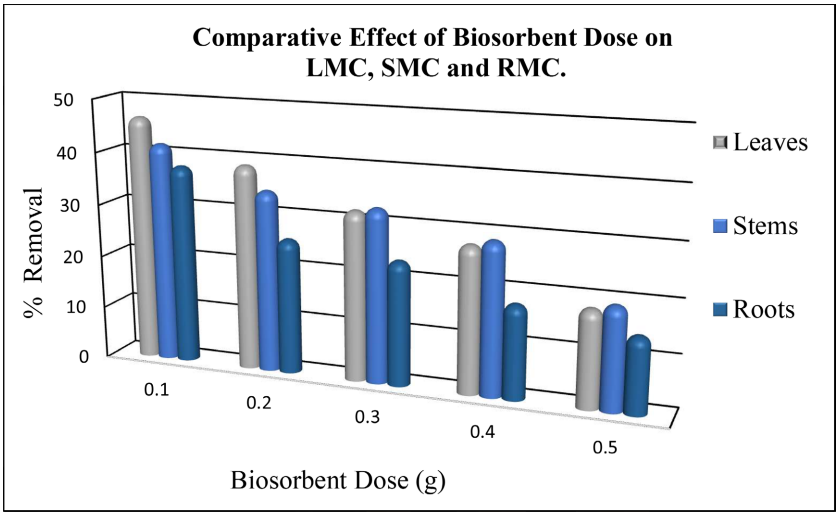

Figure 12. Comparison of percentage removal (%) of LMC, SMC and RMC on biosorbent dose.

The remarkable decrease in biosorption capacity is due to the present of concentration gradient among the biosorbent and the metal, which means with the increase in biomass quantity brings a decrease in the quantity of metal ion sorbed onto per unit weight of the biosorbent. At lower biosorbent concentration, the number of active sites is greater, with the further increase in biosorbent quantity, the biomass particles aggregated, as a result biosorption efficiency and Pb (II) uptake decreased (Ali et al., 2018).

The overall comparison of result showed in **Figure 12**. LMC (46.45%) has the greatest biosotption efficiency than SMC (41.64%) and RMC (37.67%).

3.3. Effect of Initial Metal Ions Concentration

The percentage biosorption of Pb (II) ions increased from 9.75 mg/g to 101.92 mg/g, 9.43 mg/g to 93.52 mg/g and 9.43 mg/g to 93.52 mg/g and 8.23 mg/g to 88.56 mg/g onto LMC, SMC and RMC biomass samples respectively, as shown in **Table 3**. However, the percentage removal of Pb (II) ions remarkably decreased on further increased in the initial metal ion concentrations. The removal percentage of LMC biomass has been increasing with the further increased in the initial lead ion concentration and reached the maximum removal at 100 ppm (47.62%). After that the biosorption efficiency decreased gradually with the further increased in the metal ion concentration and the minimum removal observed at 400 ppm (25.48%). Contrastingly, the adsorption capacity (q_e) gradually increased on increasing the initial lead ions concentration as shown in **Figure 13**. Similarly, the percentage removal of SMC gradually increased up to 100 ppm (41.56%) and then gradually started decreasing with the further increase in initial metal ions concentration. The adsorption capacity of SMC was increased continuously by increasing the initial lead ions concentration which can be noted in **Figure 14**. The RMC also followed a similar trend and showed the progressive increased in percentage removal for Pb (II) ions up to 100 ppm (36.85%)

Table 3. Effect of Pb (II) metal ions concentrations on adsorption capacity (q_e) and percentage removal by LMC, SMC and RMC.

	Metal Ion Conc. (ppm)	C_i (mg/L)	C_e (mg/L)	$C_i - C_e$	q_e (mg/g)	% Removal
LMC	25	25	15.25	9.75	9.75	39.00
	50	50	28.55	21.45	21.45	42.90
	100	100	52.38	47.62	47.62	47.62
	200	200	121.69	78.31	78.31	39.15
	400	400	298.08	101.92	101.92	25.48
SMC	25	25	15.57	9.43	9.43	37.72
	50	50	30.55	19.45	19.45	38.90
	100	100	58.44	41.56	41.56	41.56
	200	200	126.35	73.65	73.65	36.82
	400	400	306.48	93.52	93.52	23.38
RMC	25	25	16.77	8.23	8.23	32.92
	50	50	32.78	17.22	17.22	34.44
	100	100	63.15	36.85	36.85	36.85
	200	200	137.15	62.85	62.85	31.42
	400	400	311.44	88.56	88.56	22.14

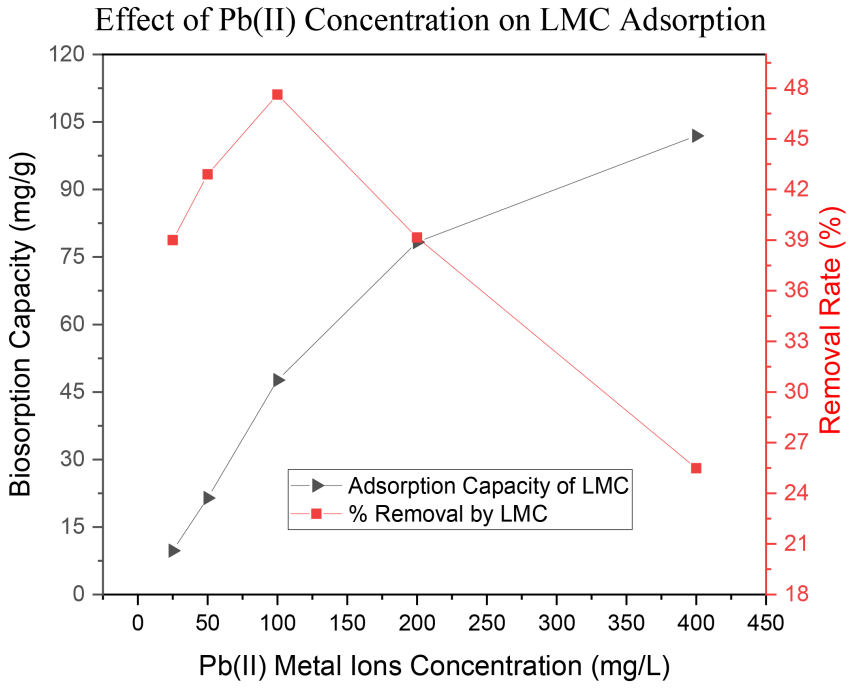

Figure 13. Effect of initial metal ions concentration of Pb (II) on the adsorption of Pb(II) by dried biomass of *Momordica charantia* leaves powder (LMC) (Experimental conditions: pH = 5, biomass dosage = 0.1 g, mixing rate = 120 rpm and contact time = 24 hours).

and after that decreased with the further increased in the initial metal ion concentration. But adsorption capacity of RMC has been increased continuously on increasing the initial lead ions concentration as seen in Figure 15. Similar trends have been reported in the biosorption of lead ions using *G. hirsutum* (cotton)

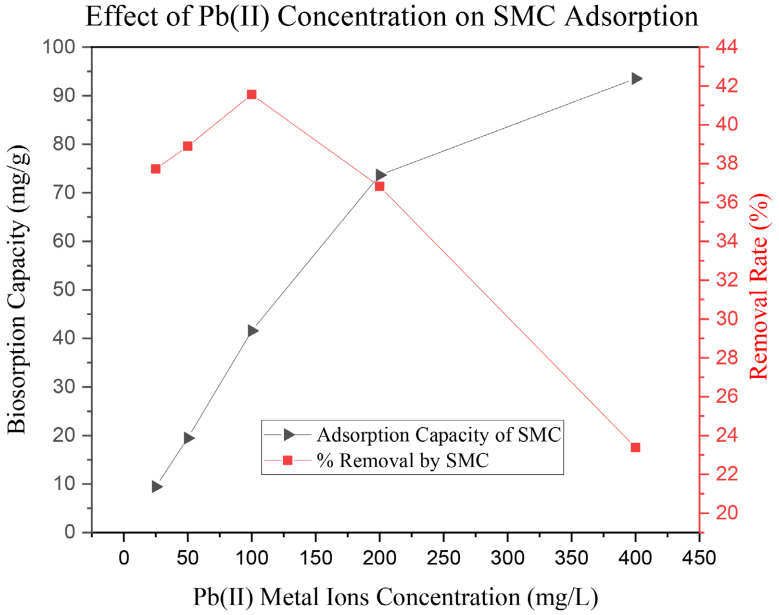

Figure 14. Effect of initial metal ions concentration of Pb (II) on the adsorption of Pb(II) by dried biomass of *Momordica charantia* stems powder (SMC) (Experimental conditions: pH = 5, biomass dosage = 0.1 g, mixing rate = 120 rpm and contact time = 24 hours).

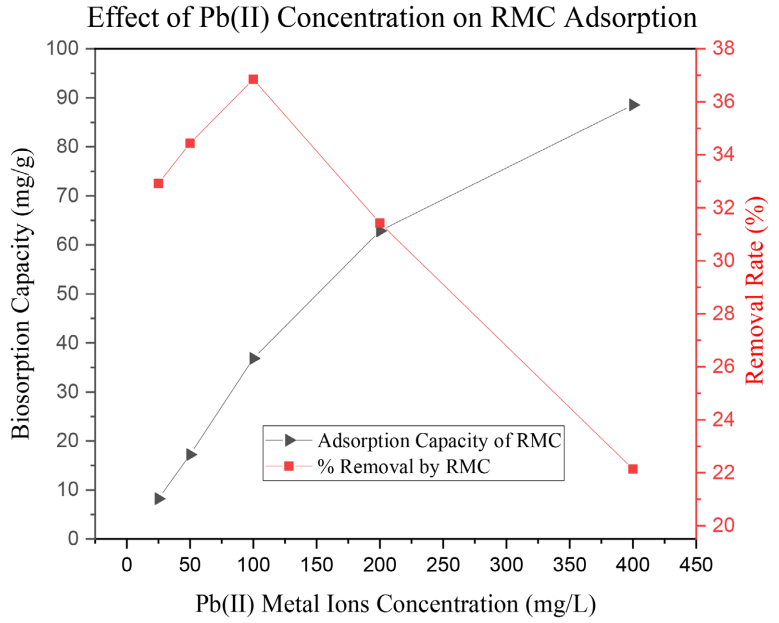

Figure 15. Effect of initial metal ions concentration of Pb (II) on the adsorption of Pb(II) by dried biomass of *Momordica charantia* roots powder (RMC) (Experimental conditions: pH = 5, biomass dosage = 0.1 g, mixing rate = 120 rpm and contact time = 24 hours).

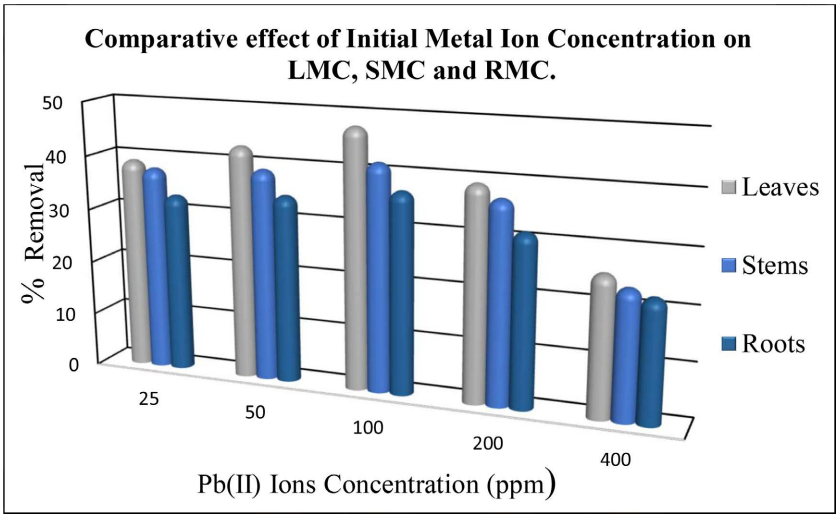

Figure 16. Comparison of percentage removal (%) of LMC, SMC and RMC on initial metal ions concentration.

biomass (Akram et al., 2019).

At 25 ppm solution there was abundant availability of active site on the material which was enough to sorbed the Pb (II) ions but as the initial concentration gradually increased the availability of active sites decreased and as a result the percentage removal decreased. The decreased in percentage removal at higher concentration is because of saturation of specific sites and area for binding, which cause lowering in the possible connection of Pb (II) ions with the present active sites of biosorbents, resulting in the decrease of removal percentage of Pb (II) ions at higher metal ion concentration.

Comparatively LMC (47.62%) has the greatest percentage removal for Pb (II) ions than SMC (41.56%) and RMC (36.85%) at 100ppm of initial lead ions concentration, as shown in **Figure 16**.

3.4. Effect of Contact Time

LMC, SMC and RMC sorption of Pb (II) ions was fast in the beginning, almost 30.28%, 28.44%, and 23.85% of metal removal takes place in first 15 minutes, respectively. The biosorption increased as the contact time increased and the maximum adsorption observed at 240 minutes 47.45%, 42.05% and 37.92% for LMC, SMC and RMC, respectively, as shown in **Figures 17-19**. Result indicates that the biosorption of Pb (II) ions were fast during the first 15 minutes, after that biosorption rate increased slowly and after 240 minutes of contact time no further considerable change in biosorption was observed, as shown in **Table 4**. This continuous increase in metal uptake and percentage removal up to 240 minutes and slower biosorption beyond this time has been discussed in the lead removal using *Mangifera indica* biomass (Nadeem et al., 2016).

Lead binding onto the biomass was rapid in the beginning. During the biosorption, the concentration of lead ions rapidly decreased. After sometimes the biosorption equilibrium is obtained; the Pb (II) ions concentration remained

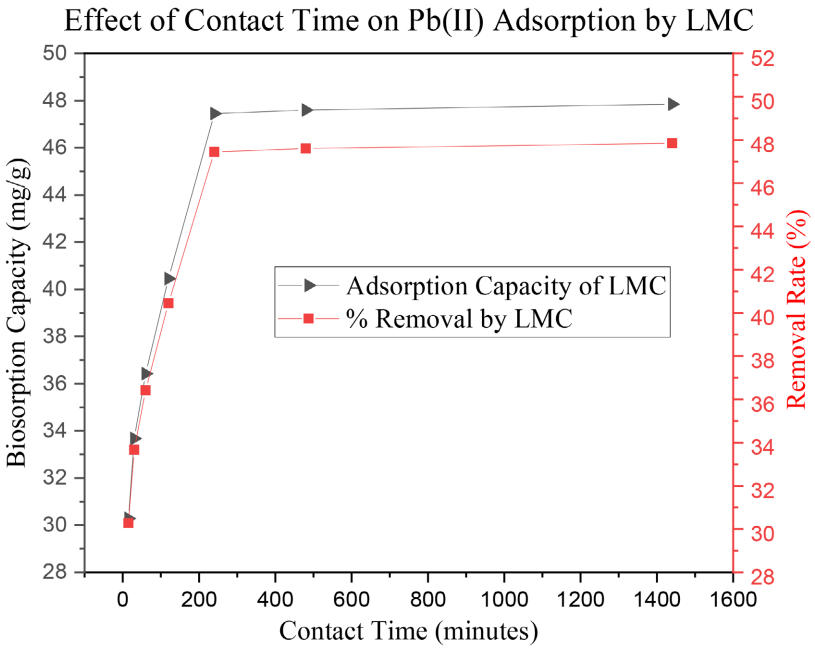

Figure 17. Effect of contact time on the biosorption of Pb (II) by *Momordica charantia* leaves powder (LMC) (Experimental conditions: pH = 5, C_i = 100 ppm, biomass dosage = 0.1 g and mixing rate = 120 rpm).

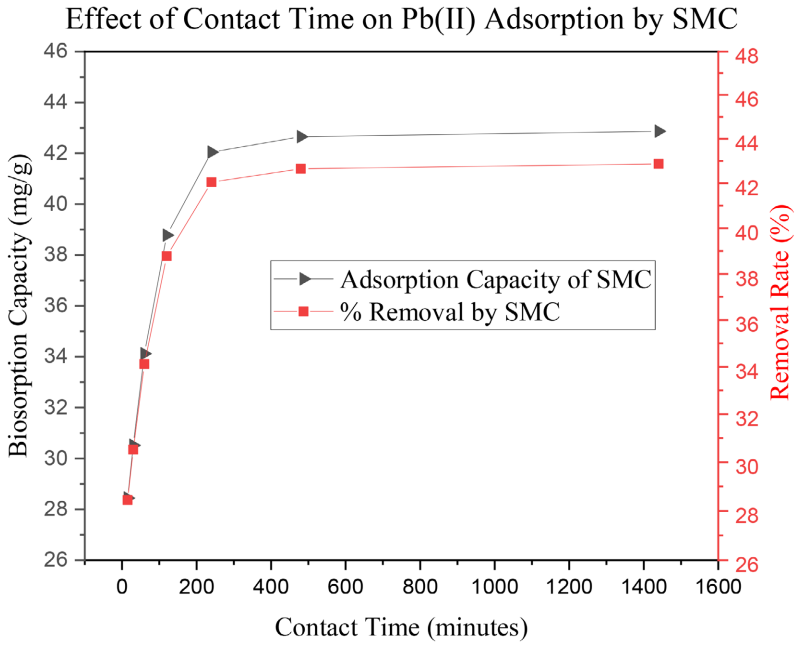

Figure 18. Effect of contact time on the biosorption of Pb (II) by *Momordica charantia* stems powder (SMC) (Experimental conditions: pH = 5, C_i = 100 ppm, biomass dosage = 0.1 g and mixing rate = 120 rpm).

same after 240 minutes remains almost constant after approximately 240 minutes. Although the biosorption process continues, the adsorbent reached the saturation stage and after that the adsorbed metal ions started desorbing into the solution. At equilibrium, there will be no significant change in the metal ions

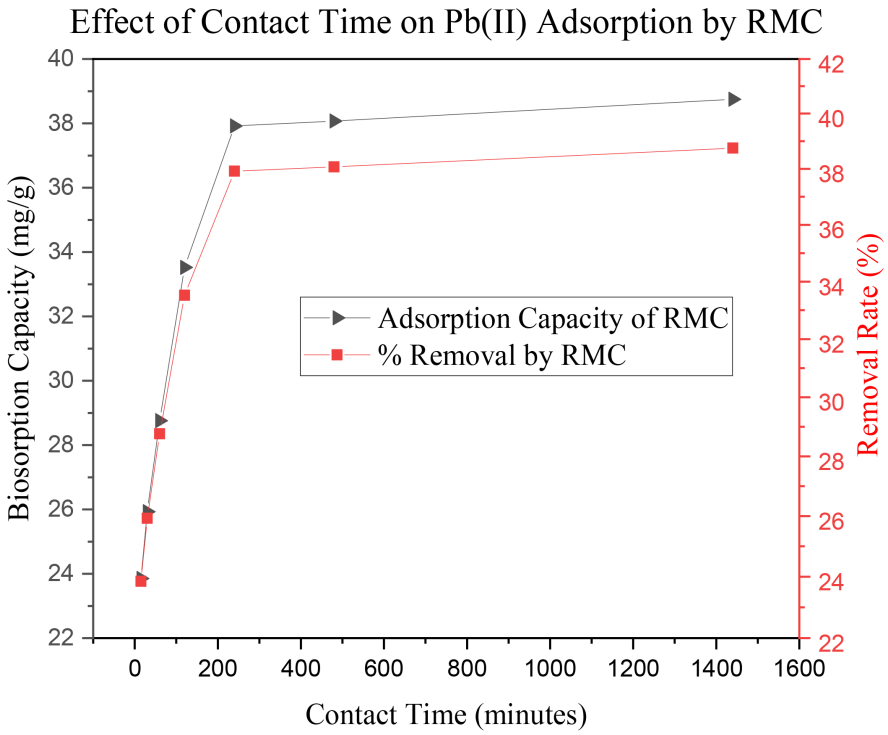

Figure 19. Effect of contact time on the biosorption of Pb (II) by *Momordica charantia* roots powder (RMC) (Experimental conditions: pH = 5, C_i = 100 ppm, biomass dosage = 0.1 g and mixing rate = 120 rpm).

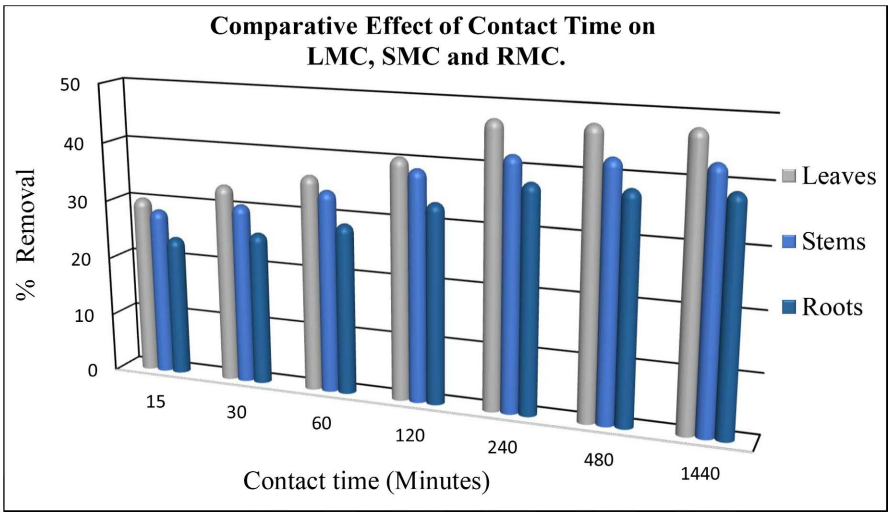

Figure 20. Comparison of percentage removal (%) of LMC, SMC and RMC on contact time.

biosorption, i.e., the adsorption rate becomes equal to the desorption rate and no net adsorption takes place. At first there are great number of active sites present on the biosorbent at which the adsorption takes place and with the passage of time it will become difficult for the ions to adsorb on the biosorbent as the forces present between the ions and adsorbent phase which have already adsorb the metal ions (Bishnoi et al., 2007).

Table 4. Effect of contact time on the adsorption capacity (q_e) and percentage removal of Pb (II) ions by LMC, SMC and RMC.

	Time (minutes)	C_i (mg/L)	C_e (mg/L)	$C_i - C_e$	q_e (mg/g)	% Removal
	15	100	69.72	30.28	30.28	30.28
	30	100	66.33	33.67	33.67	33.67
	60	100	63.58	36.42	36.42	36.42
LMC	120	100	59.55	40.45	40.45	40.45
	240	100	52.55	47.45	47.45	47.45
	480	100	52.4	47.60	47.60	47.60
	1440	100	52.15	47.85	47.85	47.85
	15	100	71.56	28.44	28.44	28.44
	30	100	69.48	30.52	30.52	30.52
	60	100	65.88	34.12	34.12	34.12
SMC	120	100	61.22	38.78	38.78	38.78
	240	100	57.95	42.05	42.05	42.05
	480	100	57.35	42.65	42.65	42.65
	1440	100	57.13	42.87	42.87	42.87
	15	100	76.15	23.85	23.85	23.85
	30	100	74.07	25.93	25.93	25.93
	60	100	71.24	28.76	28.76	28.76
RMC	120	100	66.48	33.52	33.52	33.52
	240	100	62.08	37.92	37.92	37.92
	480	100	61.93	38.07	38.07	38.07
	1440	100	61.25	38.75	38.75	38.75

The overall comparative result analysis of LMC, SMC and RMC showed in Figure 20 which indicates that LMC (47.45%) has the greatest biosorption efficiency than SMC (42.05%) and RMC (37.92%).

3.5. FTIR Analysis

The FTIR analysis was performed to find the interactions between the Pb (II) and functional groups present on the biomass. FTIR spectra of before and after biosorption were compared for LMC, SMC and RMC as shown in Figure 21, Figure 22, and Figure 23, respectively. All the types of biomasses showed many absorption peaks within the range from 4000 to 400 cm^{-1} which describes the biomass has a very complex nature. Before biosorption almost all the biomass (LMC, SMC and RMC) showed a broad absorption band in the 3600 - 3000 cm^{-1} regions, which exhibited the presence of hydroxyl group –OH (Asgher & Bhatti, 2010). The peak at approximately 2940 - 2930 cm^{-1} is due to C-H stretching of alkane (Sayyah et al., 2002). The band observed at 2400 - 2380 cm^{-1} represents

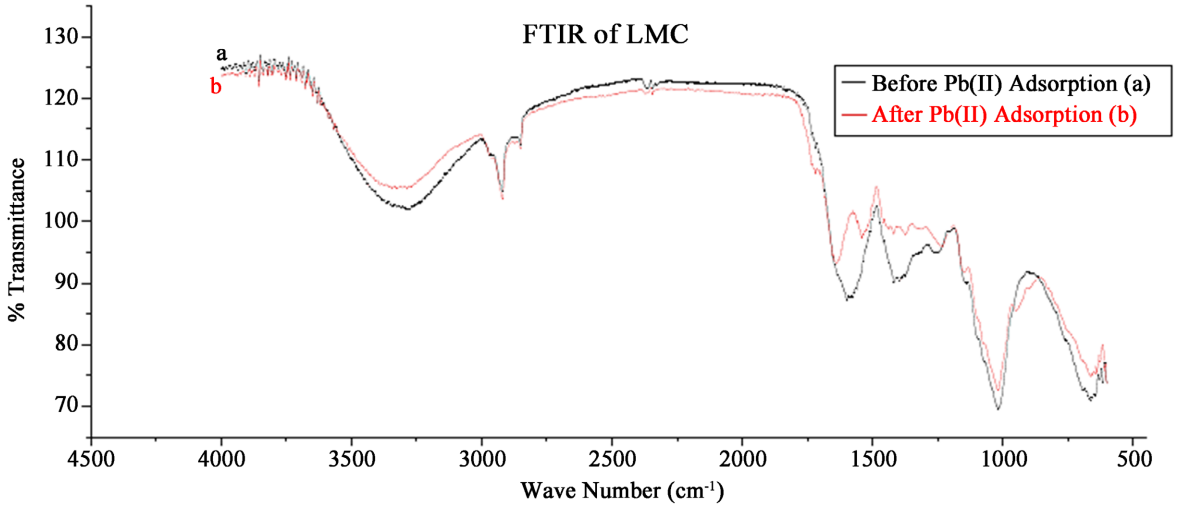

Figure 21. FTIR spectra of LMC before biosorption of Pb (II) (a) and after biosorption of Pb (II) (b).

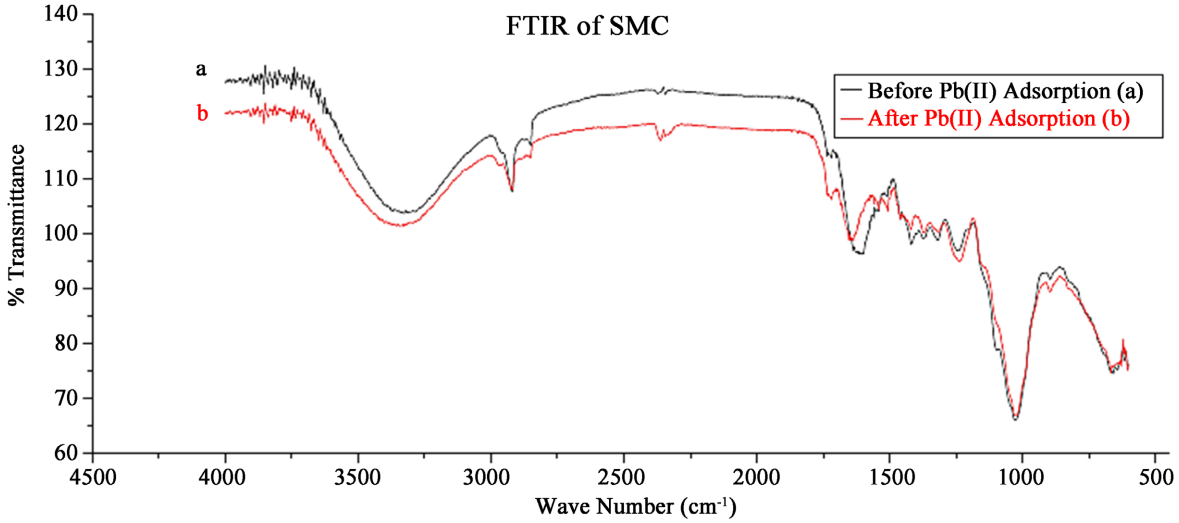

Figure 22. FTIR spectra of SMC before biosorption of Pb (II) (a) and after biosorption of Pb (II) (b).

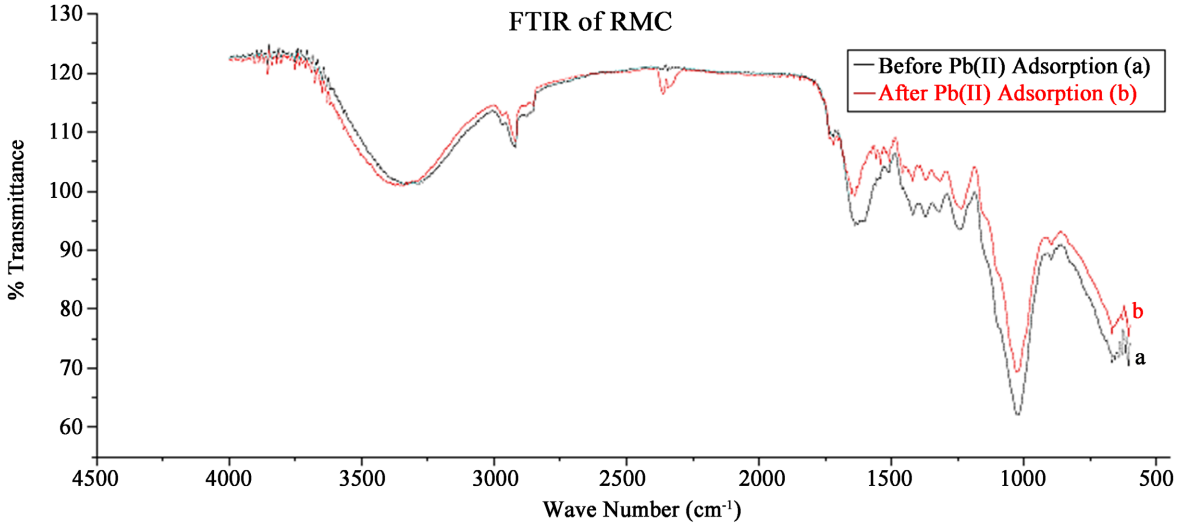

Figure 23. FTIR spectra of RMC before biosorption of Pb (II) (a) and after biosorption of Pb (II) (b).

the present of –COOH group. The peak at around 1650 - 1640 cm^{-1} is due to the stretching of C=O (Guerrero-Coronilla et al., 2014). Absorption bands at 1460 - 1420 cm^{-1} are describing the bending of –OH groups and stretching of C-O groups (Saygideger et al., 2005). The peaks around 1100 - 1080 cm^{-1} are due to the vibration of C-O-C groups. The peaks near 910 - 890 cm^{-1} may be inorganic or due to the stretching vibrations of C-C group (Amar et al., 2020). After biosorption the FTIR spectra of LMC, SMC and RMC showed the changes in the major peak and also developed some new peaks as shown in **Figure 21**, **Figure 22** and **Figure 23**, respectively, which confirmed the interaction between the Pb (II) metal and biosorbent surface. The hydroxyl group peak became broader for LMC, SMC and RMC which showed the interaction of Pb (II) metal with the –OH group. The decrease in the intensity of 2400 - 2380 cm^{-1} band was due to the replacement of hydrogen atom with the Pb (II) meta lion. The shift of peaks to 1620, 1631 and 1648 cm^{-1} for LMC, SMC and RMC, respectively, characterized by the oxidation of C = O. In addition, the considerable shift of the peaks at the region 1460 - 1420 cm^{-1} was also due to the interaction of Pb ions with –OH groups. Furthermore, the shift in the peak at 905, 911 and 912 cm^{-1} for LMC, SMC and RMC respectively showed the interaction of Pb (II) ions on the biosorbent surface. Overall FTIR results exhibited the considerable interaction among the Pb (II) ions with the hydroxyl, carbonyl, amide and ketonic functional groups of biosorbent. These functional groups are constituents of the carbohydrates, proteins and complex polymers present in LMC, SMC and RMC.

3.6. Equilibrium Isotherm Modeling:

Biosorption equilibrium is commonly explained by isotherms modeling, which are plotted between equilibrium uptake and sorbate concentration in the solution at specific temperature. There are a number of different adsorption isotherm models reported in the literature. But the Langmuir and the Freundlich isotherm models are mostly used for the adsorption equilibrium explanation (Sheha & Metwally, 2007).

3.6.1. Langmuir Isotherm

The Langmuir isotherm model helps to explain the adsorption of metal ions on the active sites present on adsorbent under isothermal conditions. It is used to explain the equilibrium association among the adsorbate and adsorbent sites (Liu, 2006). The Langmuir isotherm can be mathematically explained as:

$$\frac{C_e}{q_e} = \frac{1}{q_{\max} K_L} + \frac{C_e}{q_{\max}} \quad [3]$$

where,

C_e represents the remaining metal ions concentration at equilibrium.

q_e represents the metal ion sorbed (mg/g) at equilibrium.

$q_{\max}$ (mg/g) represents the maximum amount of ions adsorbed.

K_L represents the Langmuir adsorption isotherm constant.

The graph was plotted against C_e/q_e along with C_e. K_L and q_{max} were calculated by taking values of intercept and slope. Langmuir isotherm model have been shown for LMC, SMC and RMC in **Figures 24-26**, respectively.

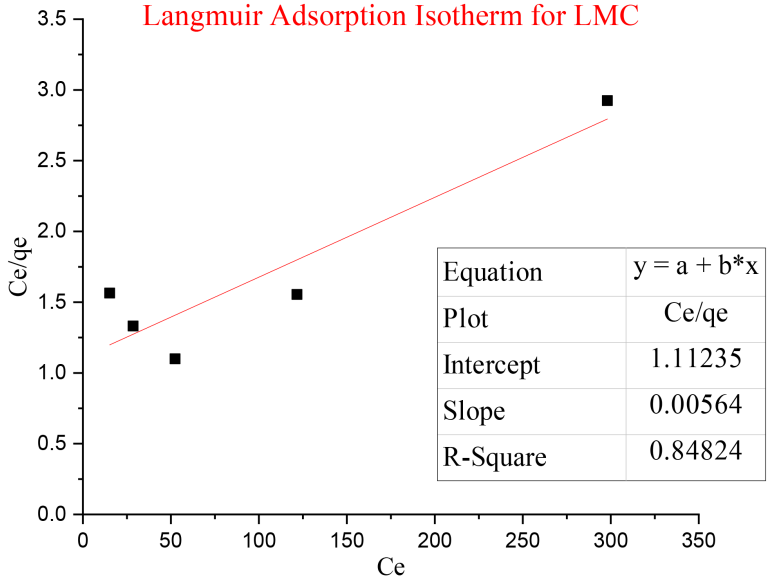

Figure 24. The Langmuir adsorption isotherm model for Pb (II) onto *Momordica charantia* leaves powder biomass (LMC). Experimental conditions: Biomass dosage = 0.1 g, pH = 5, mixing rate = 120 rpm and contact time = 24 hours at various initial Pb (II) ion concentrations.

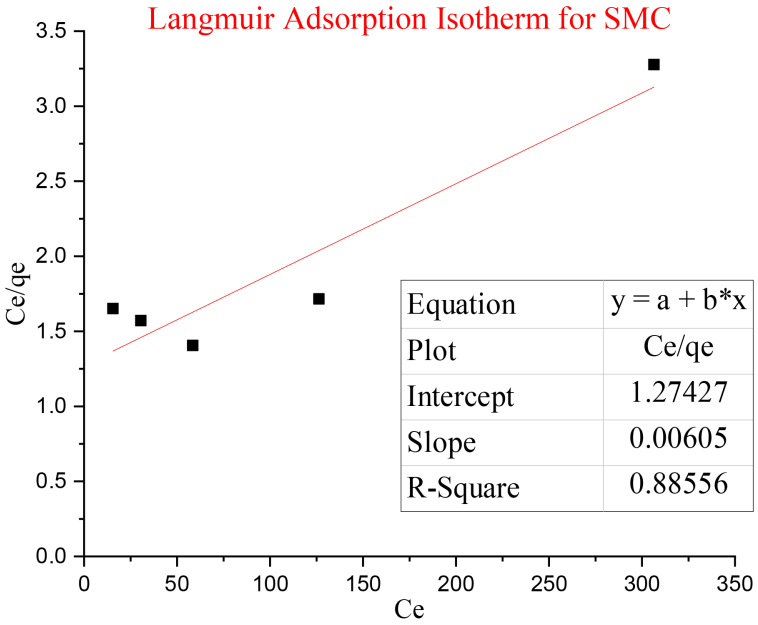

Figure 25. The Langmuir adsorption isotherm model for Pb (II) onto *Momordica charantia* stems powder biomass (SMC). Experimental conditions: Biomass dosage = 0.1 g, pH = 5, mixing rate = 120 rpm and contact time = 24 hours at various initial Pb (II) ion concentrations.

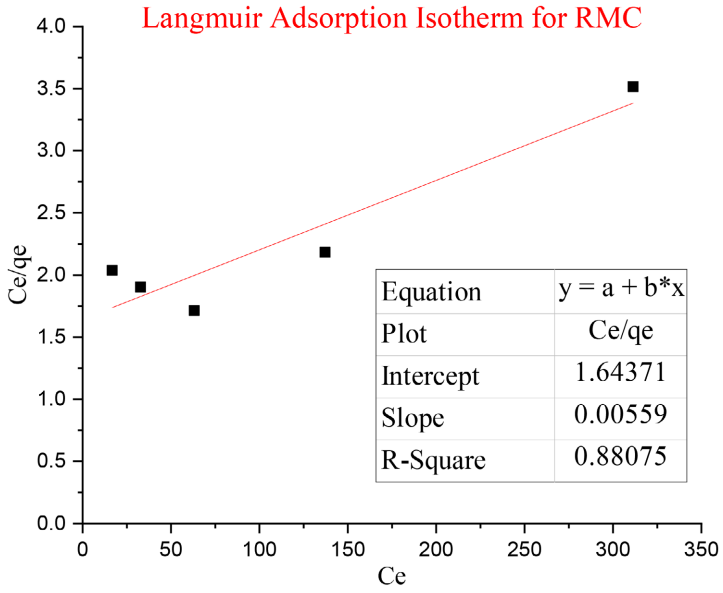

Figure 26. The Langmuir adsorption isotherm model for Pb (II) onto *Momordica charantia* roots powder biomass (RMC). Experimental conditions: Biomass dosage = 0.1 g, pH = 5, mixing rate = 120 rpm and contact time = 24 hours at various initial Pb (II) ion concentrations.

3.6.2. Freundlich Isotherm Model

Freundlich adsorption isotherm is an empirical model and yields a linear plot. The adsorbate forms both monomolecular and multimolecular layer on the adsorbent active sites (Al-Ghouti & Da'ana, 2020). The Freundlich isotherm can be expressed in the form of equation as:

$$q_e = K_F C_e^{1/n} \quad [4]$$

This equation can be arranged in linear from after taking logarithms as:

$$\log q_e = \log K_F + \frac{1}{n} \log C_e \quad [5]$$

where, C_e represents the concentration of metal ions at equilibrium (mg/L).

q_e represents the adsorbed quantity of Pb (II) at equilibrium.

K_F represents Freundlich constant.

$1/n$ is Freundlich exponent.

A graph of $\log C_e$ has plotted against log q_e. The value of $1/n$ is equivalent to the slope and K_F was calculated from the value of intercept. The graphs of Freundlich adsorption isotherm model is shown in **Figures 27-29** for LMC, SMC and RMC, respectively.

Langmuir and Freundlich isotherms parameters were calculated with the help of their respective graphs and data is shown in **Table 5**. The correlation coefficient (R^2) values were 0.8482, 0.8856 and 0.8808 for the Pb (II) adsorption for LMC, SMC and RMC, respectively were observed for Langmuir adsorption isotherm. For Freundlich adsorption isotherm the correlation coefficient (R^2) values were 0.9212, 0.9433 and 0.9617 were observed for LMC, SMC and RMC, respectively. The calculated values of R^2 were greater for the Freundlich isotherm models as compared

to Langmuir isotherm models. Hence, Freundlich isotherm model fitted best for the Pb (II) adsorption due to higher R^2 values. The maximum adsorption (q_{max}) was also investigated, which showed the highest Pb (II) uptake potential for different biomass. The order of Pb (II) uptake onto the *Momordica charantia* biomass is LMC > SMC > RMC. The R^2 and q_{max} values for Pb (II) indicated that the

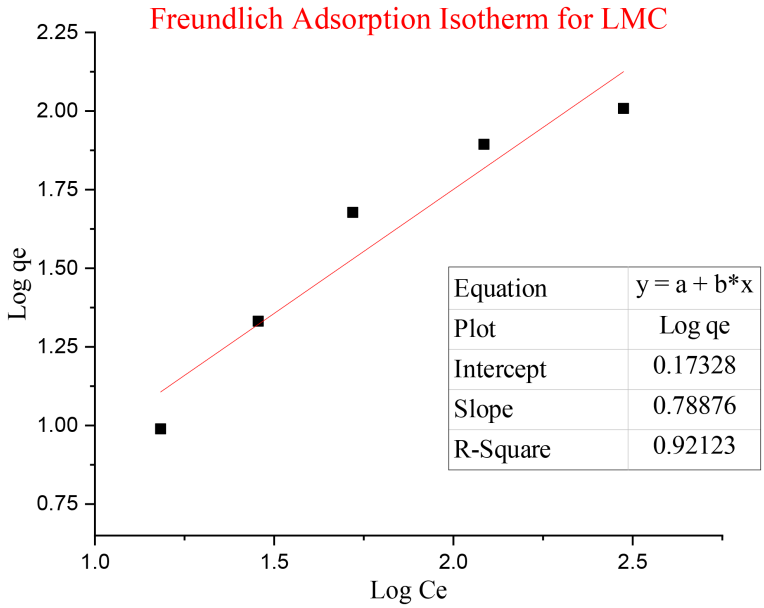

Figure 27. The Freundlich adsorption isotherm model for Pb (II) onto *Momordica charantia* leaves powder biomass (LMC). Experimental conditions: Biomass dosage = 0.1 g, pH = 5, mixing rate = 120 rpm and contact time = 24 hours at various initial Pb (II) ion concentrations.

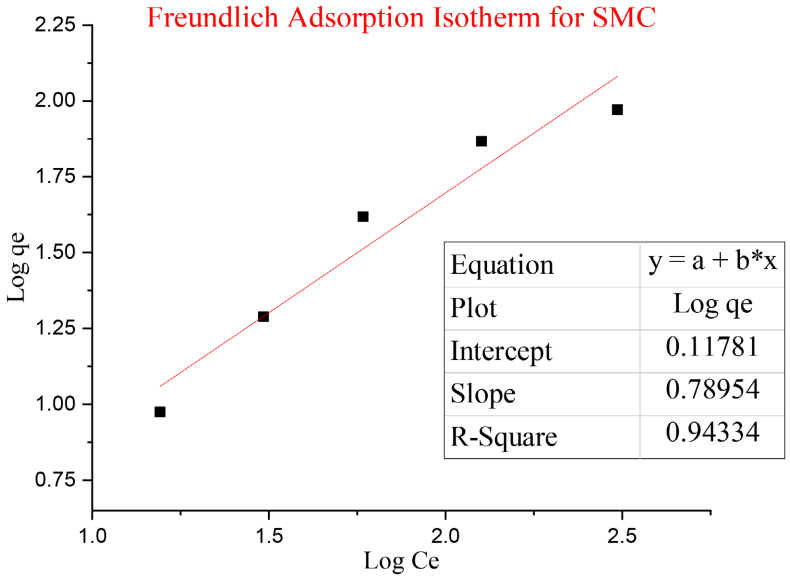

Figure 28. The Freundlich adsorption isotherm model for Pb (II) onto *Momordica charantia* stems powder biomass (SMC). Experimental conditions: Biomass dosage = 0.1 g, pH = 5, mixing rate = 120 rpm and contact time = 24 hours at various initial Pb (II) ion concentrations.

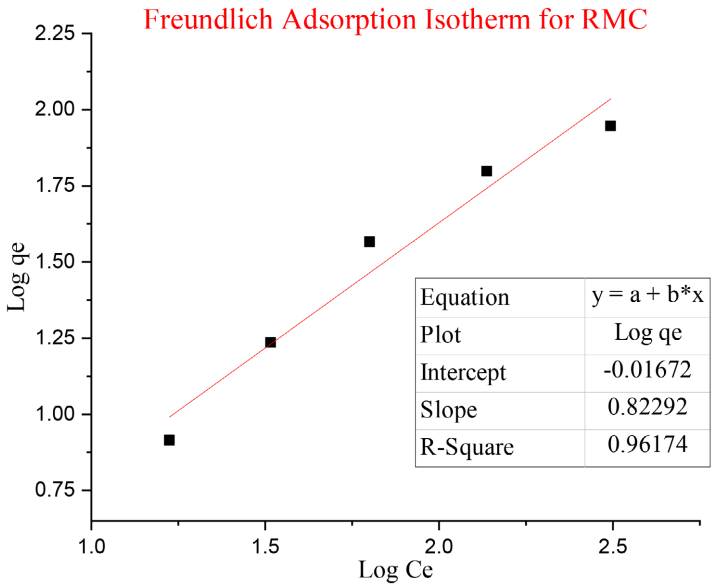

Figure 29. The Freundlich adsorption isotherm model for Pb (II) onto *Momordica charantia* roots powder biomass (RMC). Experimental conditions: Biomass dosage = 0.1 g, pH = 5, mixing rate = 120 rpm and contact time = 24 hours at various initial Pb (II) ion concentrations.

Table 5. Langmuir and Freundlich isotherms parameters for Pb (II) ions biosorption onto LMC, SMC and RMC biomass.

Biosorbent	Langmuir Isotherm Parameters			Experimental q value (mg/g)	Freundich Isotherm Parameter		
	Xm (q_{max}) mg/g	K_L mg/g	R^2		K_F (mg/g)	1/n	R^2
LMC	177.31	0.0051	0.8482	47.62	1.4903	0.7888	0.9212
SMC	165.29	0.0047	0.8856	42.36	1.3116	0.7895	0.9433
RMC	178.90	0.0034	0.8808	38.47	0.9622	0.8229	0.9617

Freundlich isotherm model demonstrated the biosorption well instead of Langmuir isotherm model. Similar investigation had been investigated in the biosorption of Pb (II) ions by *Moringa oleifera* seed powder biomass (Kowanga et al., 2016).

3.7. Kinetic Modeling

Kinetic models have been used to recognize the rate of chemical reactions. It is used to describe the speed of a reaction under different experimental conditions. Kinetics of biosorption was observed by different mathematical models. In this research work pseudo-first order and pseudo-second order kinetic model has been used.

3.7.1. Pseudo-First Order Kinetic Model

Mathematical expression of pseudo-first order kinetic model is showed in the Equation (3):

$$\log\left(q_e - q_t\right) = \log q_e - \frac{k_1 t}{2.303} \quad [6]$$

where,

q_e represent the equilibrium concentration of metal ions (mg/g).

q_t represents the adsorbed concentration of metal ions at time interval t.

k_1 known as the rate constant for pseudo-first order kinetic model.

In order to find the value of k_1, a graph is plotted against $\log(q_e - q_t)$ and time. The graphical representation of pseudo-first order reaction models are shown in Figures 30-32 for LMC, SMC and RMC, respectively.

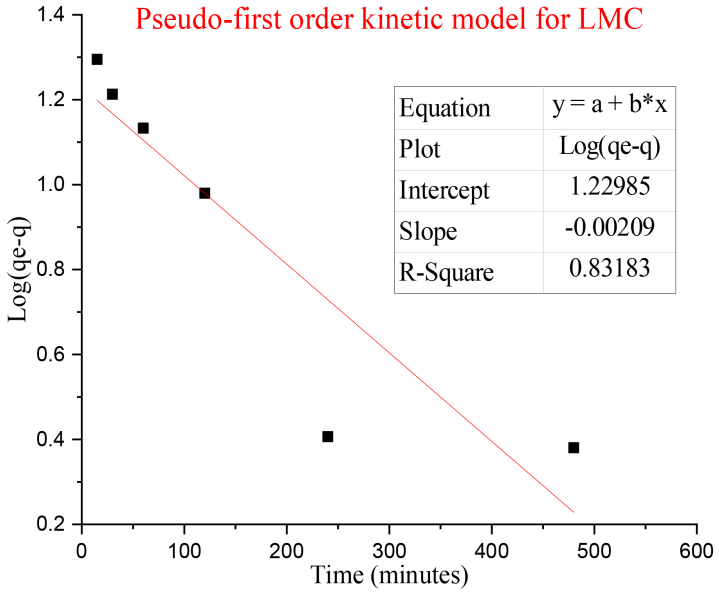

Figure 30. Pseudo-first order kinetics model for the adsorption of Pb (II) onto *Momordica charantia* leaves powder biomass (LMC). Experimental Conditions: C_i = 100 ppm, pH = 5.0, biomass dose = 0.1 g, mixing rate = 120 rpm at different intervals of time.

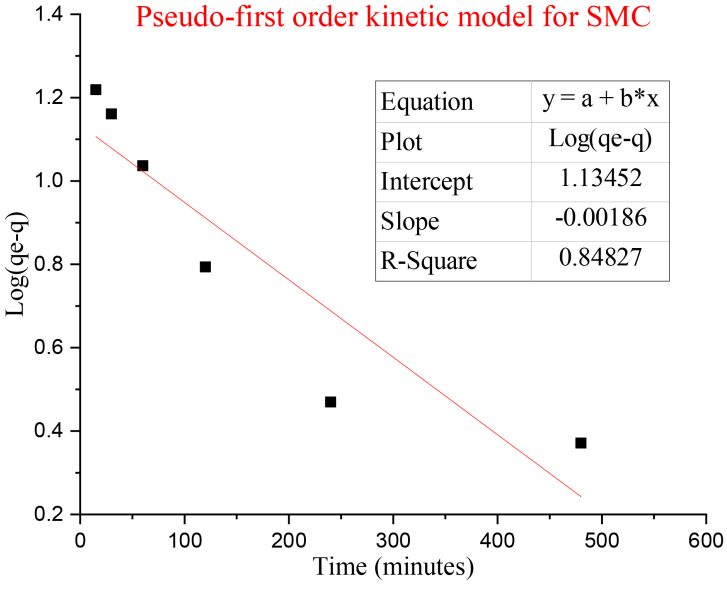

Figure 31. Pseudo-first order kinetics model for the adsorption of Pb (II) onto *Momordica charantia* stems powder biomass (SMC). Experimental Conditions: C_i = 100 ppm, pH = 5.0, biomass dose = 0.1 g, mixing rate = 120 rpm at different intervals of time.

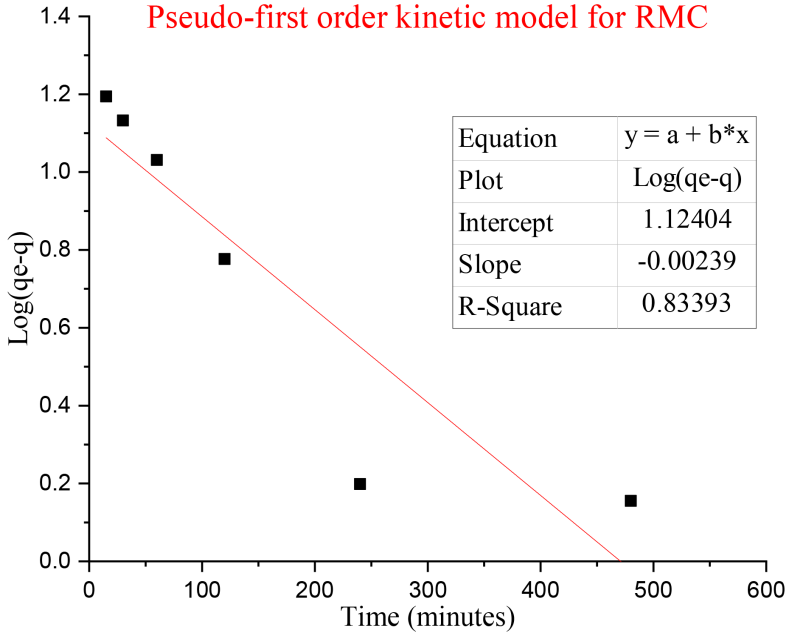

Figure 32. Pseudo-first order kinetics model for the adsorption of Pb (II) onto *Momordica charantia* roots powder biomass (RMC). Experimental Conditions: C_i = 100 ppm, pH = 5.0, biomass dose = 0.1 g, mixing rate = 120 rpm at different intervals of time.

3.7.2. Pseudo-Second Order Kinetic Model

Mathematical derivation of pseudo-second order kinetic model is explained as:

$$\frac{t}{q_t} = \frac{1}{k_2 q_e^2} + \frac{1}{q_e} t \qquad [7]$$

where,

q_e represent the adsorption at equilibrium stage (mg/g).

q_t represents the biosorption at time interval t.

k_2 is the rate constant for pseudo-second order kinetic model.

For pseudo-second order reaction a graph is plotted between t/q and t. The graphical representation of pseudo-second order reaction models are shown in Figures 33-35 for LMC, SMC and RMC, respectively.

The comparison between the pseudo-first and the pseudo-second order kinetic model is shown in Table 6. The values of k_1 and k_2 obtained by using the graphs of pseudo-first order and pseudo-second order kinetic model, respectively and the correlation coefficient (R^2) value of Pb (II) biosorption onto LMC, SMC and RMC biomass for pseudo-first order were 0.8318, 0.8483 and 0.8339, respectively. While, pseudo-second order kinetic model showed the greater value of correlation coefficient; 0.9998, 0.9999 and 0.9999 for LMC, SMC and RMC, respectively. Due to higher R^2 value pseudo-second order kinetic model fitted best for the adsorption of Pb (II) by LMC, SMC and RMC. The removal rate of Pb (II) increases as the contact time increases till equili-

brium was reached. Also, the q_e values for pseudo-second order kinetic model also correlates with the observed experimental values. Similar behavior of Pb (II) adsorption had been reported onto *Mangifera indica* (Mango) waste biomass (Nadeem et al., 2016).

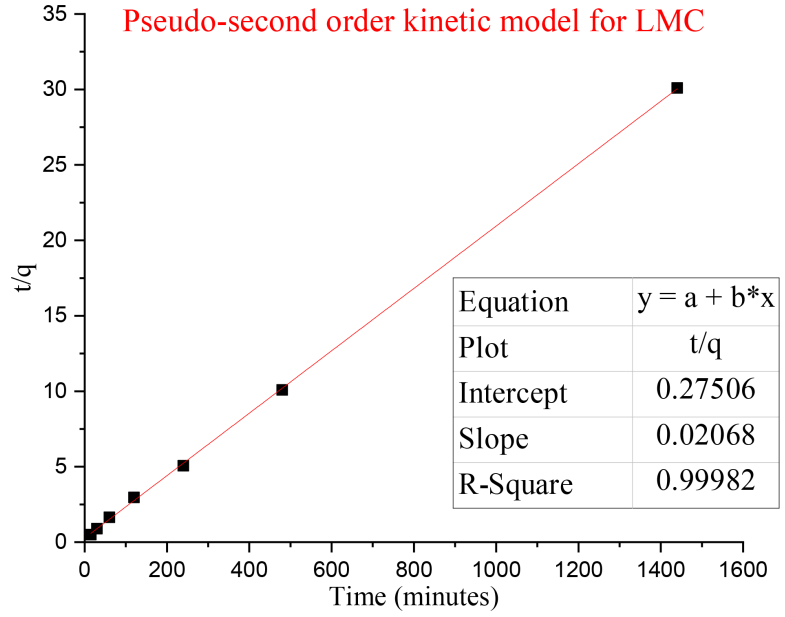

Figure 33. Pseudo-second order kinetics model for the adsorption of Pb (II) onto *Momordica charantia* leaves powder biomass (LMC). Experimental Conditions: C_i = 100 ppm, pH = 5.0, biosorbent dose = 0.1 g, mixing rate = 120 rpm at different intervals of time.

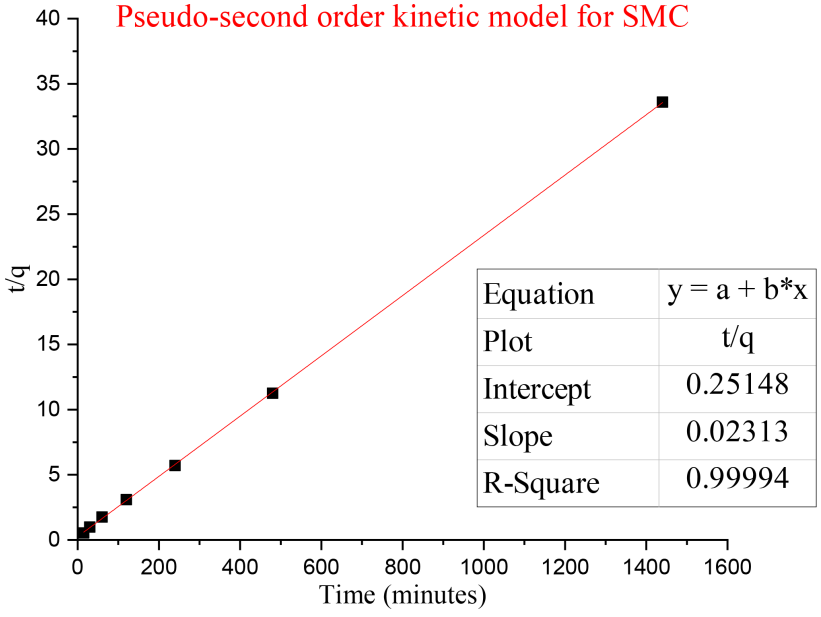

Figure 34. Pseudo-second order kinetics model for the adsorption of Pb (II) onto *Momordica charantia* stems powder biomass (SMC). Experimental Conditions: C_i = 100 ppm, pH = 5.0, biosorbent dose = 0.1 g, mixing rate = 120 rpm at different intervals of time.

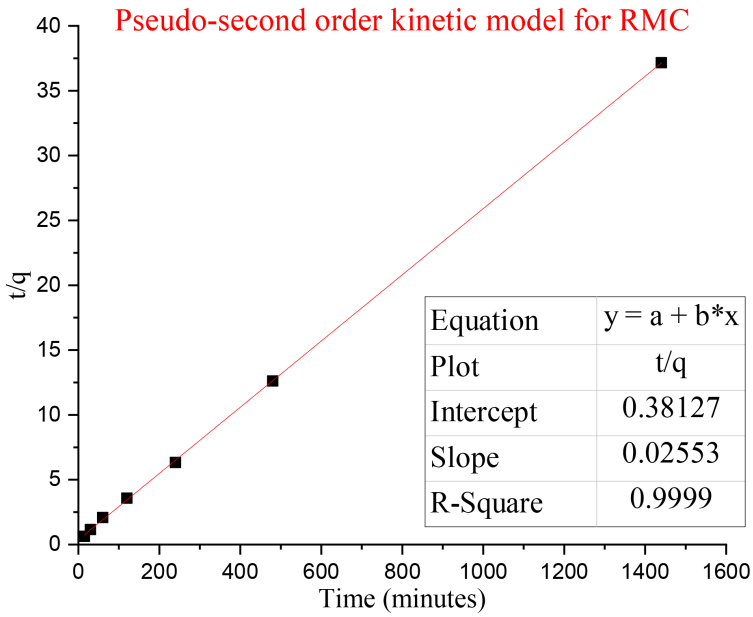

Figure 35. Pseudo-second order kinetics model for the adsorption of Pb (II) onto *Momordica charantia* roots powder biomass (RMC). Experimental Conditions: C_i = 100 ppm, pH = 5.0, biosorbent dose = 0.1 g, mixing rate = 120 rpm at different intervals of time.

Table 6. Pseudo-first order and pseudo-second order kinetic model for Pb (II) biosorption onto LMC, SMC and RMC biomass.

Biosorbent	Pseudo-first Order Kinetic Model			Pseudo-second Order Kinetic Model		
	q_e mg/g	k_1	R^2	q_e mg/g	k_2	R^2
LMC	16.98	0.0048	0.8318	48.56	0.0016	0.9998
SMC	13.63	0.0043	0.8483	43.23	0.0047	0.9999
RMC	13.31	0.0055	0.8339	39.17	0.0017	0.9999

4. Conclusion

The comparative result showed that LMC (47.62) has the highest biosorption potential for the elimination of Pb (II) ions followed by SMC (42.36) and finally by the RMC (38.47). Freundlich isotherm model suited better than Langmuir isotherm model with the R^2 calculated as 0.9212, 0.9433 and 0.9617, for LMC, SMC and RMC, respectively. Kinetic studies showed the pseudo-second-order model was best fitted in defining the kinetics of the biosorption of lead ions onto the bitter gourd biomass with the R^2 value of 0.9998, 0.9999 and 0.9999, for LMC, SMC and RMC, respectively. Results indicated that adsorption capacity gradually decreased with the increase of adsorbent dose and gradually increased with the increase in initial Pb (II) ions concentration. The results reported during this research work showed that the bitter gourd could be utilized as a good biosorbent for the biosorption of Pb (II) ions from polluted water.

Conflicts of Interest

The authors declare no conflicts of interest regarding the publication of this paper.

References

Abbas, S. H., Ismail, I. M., Mostafa, T. M., & Sulaymon, A. H. (2014). Biosorption of Heavy Metals: A Review. *Journal of Chemical Science and Technology, 3,* 74-102.

Ahluwalia, S. S., & Goyal, D. (2007). Microbial and Plant Derived Biomass for Removal of Heavy Metals from Wastewater. *Bioresource Technology, 98,* 2243-2257. https://doi.org/10.1016/j.biortech.2005.12.006

Akpor, O. B., & Muchie, B. (2011). Environmental and Public Health Implications of Wastewater Quality. *African Journal of Biotechnology, 10,* 2379-2387.

Akram, M., Khan, B., Imran, M., Ahmad, I., Ajaz, H., Tahir, M. et al. (2019). Biosorption of Lead by Cotton Shells Powder: Characterization and Equilibrium Modeling Study. *International Journal of Phytoremediation, 21,* 138-144. https://doi.org/10.1080/15226514.2018.1488810

Al-Ghouti, M. A., & Da'ana, D. A. (2020). Guidelines for the Use and Interpretation of Adsorption Isotherm Models: A Review. *Journal of Hazardous Materials, 393,* Article 122383. https://doi.org/10.1016/j.jhazmat.2020.122383

Ali, M. E., Abd El-Aty, A. M., Badawy, M. I., & Ali, R. K. (2018). Removal of Pharmaceutical Pollutants from Synthetic Wastewater Using Chemically Modified Biomass of Green Alga *Scenedesmus obliquus*. *Ecotoxicology and Environmental Safety, 151,* 144-152. https://doi.org/10.1016/j.ecoenv.2018.01.012

Amar, M. B., Walha, K., & Salvadó, V. (2020). Evaluation of Olive Stones for Cd(II), Cu(II), Pb(II) and Cr(VI) Biosorption from Aqueous Solution: Equilibrium and Kinetics. *International Journal of Environmental Research, 14,* 193-204. https://doi.org/10.1007/s41742-020-00246-5

Asgher, M., & Bhatti, H. N. (2010). Mechanistic and Kinetic Evaluation of Biosorption of Reactive Azo Dyes by Free, Immobilized and Chemically Treated *Citrus sinensis* Waste Biomass. *Ecological Engineering, 36,* 1660-1665. https://doi.org/10.1016/j.ecoleng.2010.07.003

Ashraf, M. A., Maah, M. J., & Yusoff, I. (2011). Heavy Metals Accumulation in Plants Growing in ex tin Mining Catchment. *International Journal of Environmental Science & Technology, 8,* 401-416. https://doi.org/10.1007/BF03326227

Bawuro, A. A., Voegborlo, R. B., & Adimado, A. A. (2018). Bioaccumulation of Heavy Metals in Some Tissues of Fish in Lake Geriyo, Adamawa State, Nigeria. *Journal of Environmental and Public Health, 2018,* Article ID: 1854892. https://doi.org/10.1155/2018/1854892

Beni, A. A., & Esmaeili, A. (2020). Biosorption, an Efficient Method for Removing Heavy Metals from Industrial Effluents: A Review. *Environmental Technology & Innovation, 17,* Article 100503. https://doi.org/10.1016/j.eti.2019.100503

Bishnoi, N. R., Kumar, R., & Bishnoi, K. (2007). Biosorption of Cr(VI) with *Trichoderma viride* Immobilized Fungal Biomass and Cell Free Ca-Alginate Beads. *Indian Journal of Experimental Biology, 45,* 657-664.

Chaney, R., & Mielke, H. (1986). Standard for Soil Lead Limitations in the United States, Trace Substance. *Environmental Health, 20,* 358.

Guerrero-Coronilla, I., Morales-Barrera, L., Villegas-Garrido, T. L., & Cristiani-Urbina,

E. (2014). Biosorption of Amaranth Dye from Aqueous Solution by Roots, Leaves, Stems and the Whole Plant of *E. crassipes*. *Environmental Engineering & Management Journal (EEMJ), 13*. https://doi.org/10.30638/eemj.2014.212

Gurugubelli, B., Pervez, S., & Tiwari, S. (2013). Characterization and Spatiotemporal Variation of Urban Ambient Dust Fallout in Central India. *Aerosol and Air Quality Research, 13,* 83-96. https://doi.org/10.4209/aaqr.2012.06.0141

Kowanga, K. D., Gatebe, E., Mauti, G. O., & Mauti, E. M. (2016). Kinetic, Sorption Isotherms, Pseudo-First-Order Model and Pseudo-Second-Order Model Studies of Cu(II) and Pb(II) Using Defatted *Moringa oleifera* Seed Powder. *The Journal of Phytopharmacology, 5,* 71-78. https://doi.org/10.31254/phyto.2016.5206

Liu, Y. (2006). Some Consideration on the Langmuir Isotherm Equation. *Colloids and Surfaces A: Physicochemical and Engineering Aspects, 274,* 34-36. https://doi.org/10.1016/j.colsurfa.2005.08.029

Manzoor, Q., Sajid, A., Hussain, T., Iqbal, M., Abbas, M., & Nisar, J. (2019). Efficiency of Immobilized *Zea mays* Biomass for the Adsorption of Chromium from Simulated Media and Tannery Wastewater. *Journal of Materials Research and Technology, 8,* 75-86. https://doi.org/10.1016/j.jmrt.2017.05.016

Munichandran, M., Gangadhar, B., & Naidu, G. R. K. (2016). Bioremoval of Nickel and Lead Using Bitter Gourd (*Momordica charantia*) Seeds. *International Journal of Advanced Research in Science, Engineering and Technology, 3,* 2475-2484.

Nadeem, R., Manzoor, Q., Iqbal, M., & Nisar, J. (2016). Biosorption of Pb(II) onto Immobilized and Native *Mangifera indica* Waste Biomass. *Journal of Industrial and Engineering Chemistry, 35,* 185-194. https://doi.org/10.1016/j.jiec.2015.12.030

Padmavathy, K. S., Madhu, G., & Haseena, P. V. (2016). A Study on Effects of pH, Adsorbent Dosage, Time, Initial Concentration and Adsorption Isotherm Study for the Removal of Hexavalent Chromium (Cr(VI)) from Wastewater by Magnetite Nanoparticles. *Procedia Technology, 24,* 585-594. https://doi.org/10.1016/j.protcy.2016.05.127

Saygideger, S., Gulnaz, O., Istifli, E. S., & Yucel, N. (2005). Adsorption of Cd(II), Cu(II) and Ni (II) Ions by *Lemna minor* L.: Effect of Physicochemical Environment. *Journal of Hazardous Materials, 126,* 96-104. https://doi.org/10.1016/j.jhazmat.2005.06.012

Sayyah, S. M., Khalil, A. B., & Ghazy, M. B. (2002). Some Aspects on the Constitution of Egyptian Eichhornia Crassipesphenol Polycondensate Resins. *International Journal of Polymeric Materials, 51,* 981-1004. https://doi.org/10.1080/714975688

Sheha, R. R., & Metwally, E. (2007). Equilibrium Isotherm Modeling of Cesium Adsorption onto Magnetic Materials. *Journal of Hazardous Materials, 143,* 354-361. https://doi.org/10.1016/j.jhazmat.2006.09.041

Sprocati, A. R., Alisi, C., Segre, L., Tasso, F., Galletti, M., & Cremisini, C. (2006). Investigating Heavy Metal Resistance, Bioaccumulation and Metabolic Profile of a Metallophile Microbial Consortium Native to an Abandoned Mine. *Science of the Total Environment, 366,* 649-658. https://doi.org/10.1016/j.scitotenv.2006.01.025

Talaro, K. P., & Talaro, A. (2002). *Foundations in Microbiology*. McGraw-Hill College.

UNICEF (2018). *Levels and Trends in Child Malnutrition*. https://www.mheducation.com/highered/product/talaro-s-foundations-microbiology-chess/M9781260259025.html

Vijayaraghavan, K., & Yun, Y. S. (2008). Bacterial Biosorbents and Biosorption. *Biotechnology Advances, 26,* 266-291. https://doi.org/10.1016/j.biotechadv.2008.02.002

Vishwanath, P. M., Pandey, P., & Bhargava, A. (2017). Water Pollution-Global Perspec-

tive with Special Reference to India. *JBINO, 6,* 853-863.

Volesky, B. (1990). Biosorption and Biosorbents. In B. Volesky (Ed.), *Biosorption of Heavy Metals* (pp. 3-5). Boca Raton: CRC Press.